Indian J Med Res 155, January 2022, pp 178-88
DOI: 10.4103/ijmr.IJMR_677_21

Quick Response Code:

Pathological findings in COVID-19: A conventional autopsy-based study from India

Hetal C. Kyada[1], Rohit V. Bhalara[2], Divyesh K. Vadgama[1], Pratik R. Varu[1], Mahesh M. Trangadia[1], Prince J. Manvar[1] & Shailesh D. Bhuva[1]

Departments of [1]Forensic Medicine & [2]Pathology, Pandit Deendayal Upadhyay Government Medical College, Civil Hospital Campus, Rajkot, Gujarat, India

Received March 5, 2021

***Background & objectives*: Autopsy study has been considered the gold standard method for studying the effects of any disease on the body. Since COVID-19 is a novel disease, autopsy is crucial to understand its pathophysiology. This study was conducted to analyze the microscopic and macroscopic findings of various organs in COVID-19 and to associate those findings with clinical observations and laboratory findings.**

***Methods*: Conventional invasive autopsies were performed on 33 patients with COVID-19 from September 7, 2020 to December 23, 2020. All the organs were removed by routine dissection techniques and preserved in 10 per cent formalin. The tissues were processed and stained according to standard practices using haematoxylin-eosin (H & E) and periodic acid-schiff (PAS) stain.**

***Results*: The study included 28 males and 5 females with a median age of 61 yr (range 30-90 yr). Massive pulmonary oedema and thrombi in the lungs were the characteristic features macroscopically. On microscopic examination, diffuse alveolar damage in the exudative/proliferative phase was found in 29 (87.88%) cases. Among the other notable microscopic findings were bronchopneumonia and lung abscesses due to secondary bacterial infection (n=17, 51.52%), acute tubular injury (n=21, 63.64%) and thrombi in the lungs, heart, and kidneys.**

***Interpretation & conclusions*: COVID-19 primarily affected the respiratory and the renal systems in the vast majority of severely affected patients in our study. We also found signs of hypercoagulability, as evidenced by widespread thrombi in multiple organs, along with a raised d-dimer level and a hyperinflammatory state manifested by elevated inflammatory markers. Our autopsy findings and altered laboratory investigations support the role of immune-mediated cellular injury along with direct virus-mediated cellular damage.**

Key words Acute tubular injury - autopsy - diffuse alveolar damage - hypercoagulability - hyperinflammatory state - SARS-CoV-2 - thrombi

There have been many studies conducted worldwide to understand the virology, epidemiology, pathogenesis, diagnosis, treatment, and vaccine development of SARS-CoV-2[1,2]. Despite this, autopsy

studies exploring its effects on different organs of the body were relatively few since there was a higher risk of disease transmission. Since autopsy is considered the gold standard method for studying effects of any disease on the body, it could play a crucial role in COVID-19 as well[3,4]. There have been a few such studies conducted worldwide that have shed light on the effects of SARS-CoV-2 in the body[5-15]. This study was conducted to analyse the multi-organ pathology of 33 patients who died with COVID-19 and their relation to clinical and laboratory findings. The relationship between autopsy findings and the duration of illness was also examined and microbial culture was done to determine the presence of a secondary infection.

Material & Methods

Conventional invasive autopsies were performed on 33 patients who died with COVID-19 at the department of Forensic Medicine, Pandit Deendayal Upadhyay Government Medical College, Rajkot, Gujarat (India), from September 7 to December 23, 2020. SARS-CoV-2 infection was confirmed by the Indian Council of Medical Research (ICMR) approved testing methods[16] before or on admission to the hospital in all patients. Sixteen of the 33 patients were diagnosed by RT-PCR of nasopharyngeal and oropharyngeal swabs. The remaining 17 were diagnosed using rapid antigen tests (RAT) of nasopharyngeal swabs.

The study was initiated after approval from the Ethics Committee of our institute. A written informed consent was obtained from the next of kin. Demographic, clinical and other pertinent data about the patients were gathered from hospital records.

In all cases, autopsies were performed in accordance with the COVID-19 guidelines on dead body management issued by the Ministry of Health and Family Welfare, Government of India[17], as well as guidelines by the ICMR[18]. To reduce the risk of transmission of SARS-CoV-2, autopsies were carried out in a separate autopsy room with airflow control. All necessary airborne infection control methods were strictly followed. Complete autopsy was performed and organs were removed following routine dissection techniques with precautions to prevent the generation of aerosols. Whole brain, both lungs, heart, a piece of liver, half of the spleen and half of each kidney were preserved in 10 per cent buffered formalin for three days as suggested by the Centers for Disease Control and Prevention (CDC) guidelines[19] and practice, followed by other researchers[5,10]. The tissues were processed according to the standard practices in our histopathology laboratory and stained with haematoxylin & eosin (H & E). Besides H and E, periodic acid-Schiff (PAS) stain was utilized for renal tissues.

A piece of lung and pleural fluid were collected separately in sterile containers for culture. The blood was collected in a culture bottle containing brain heart infusion (BHI) broth supplemented with 0.05 per cent sodium polyanethol sulfonate (SPS). The samples were collected with the utmost care to avoid contamination, and were sent to the microbiology laboratory of our institute without delay.

For each patient, the duration of illness was calculated from the onset of COVID-19 symptoms until death to correlate with microscopic findings.

Results

The study included 28 males (84.85%) and five females (15.15%) with a median age of 61 yr (range 30-90 yr). The median duration of illness was 12 days (range 3-21 days). The median duration of hospitalization was seven days (range 1-17 days). The average interval between death to autopsy was three hours. Table I summarizes the demographic characteristics of patients, the interval from death to autopsy, the duration of illness, the duration of hospitalization, the duration of mechanical ventilation and the histological findings in the lung *i.e.* phase of diffuse alveolar damage (DAD).

The most common clinical presentation at the time of hospitalization was breathlessness (28 patients, 84.85%), followed by fever (21 patients, 63.64%) and cough (17 patients, 51.52%). Less common clinical presentations were chills (4 patients, 12.12%), common cold (3 patients, 9.09%), weakness (3 patients, 9.09%), vomiting (2 patients, 6.06%), body ache (2 patients, 6.06%), dryness of mouth (1 patient, 3.03%), diarrhoea (1 patient, 3.03%), sore throat (1 patient, 3.03%), convulsions (1 patient, 3.03%) and unconsciousness (1 patient, 3.03%).

Data on co-morbidities were available for 26 patients. Among these 26 patients, four had no co-morbidities (15.38%), three had hypertension (11.54%), five had diabetes mellitus (19.23%), and one each had suspected interstitial lung disease – asbestosis, and neurocysticercosis. Other patients suffered from multiple co-morbidities. Diabetes mellitus

Table I. Demographic characteristics of patients (n=33), interval from death to autopsy, duration of illness, duration of hospitalization, duration of mechanical ventilation and phase of diffuse alveolar damage (DAD)

Sex	Age (yr)	Interval from death to autopsy (h and min)	Duration of illness (days)	Duration of hospitalization (days)	Duration of mechanical ventilation (days)	Exudative/ proliferative DAD
Male	85	03:00	11	2	0	Proliferative
Male	67	03:00	5	1	2	Exudative
Male	59	04:30	11	10	8	Proliferative
Male	30	04:10	13	8	3	Proliferative
Female	90	02:30	5	4	2	Exudative
Male	61	01:45	14	10	6	Proliferative
Male	59	03:40	21	7	3	Proliferative
Male	86	05:00	12	2	0	Proliferative
Male	58	01:00	9	2	3	Exudative
Female	80	03:00	19	13	12	Proliferative
Male	65	02:25	10	9	3	Exudative
Male	66	01:45	6	3	1	Exudative
Male	65	03:45	6	2	2	None
Male	70	02:35	12	11	2	Proliferative
Male	80	02:30	16	13	3	Proliferative
Male	65	03:45	3	1	1	None
Male	70	03:35	13	11	8	Proliferative
Male	77	04:05	12	9	2	Proliferative
Male	76	03:15	14	10	10	Proliferative
Male	58	03:10	19	17	16	Proliferative
Male	80	01:15	9	7	3	Exudative
Male	50	02:00	8	4	1	Proliferative
Male	55	01:35	13	10	8	Proliferative
Male	38	03:00	6	4	2	Exudative
Male	63	01:55	13	9	9	Proliferative
Male	47	06:10	15	7	8	Proliferative
Female	36	02:25	21	3	0	None
Male	55	02:40	7	4	4	Proliferative
Female	52	03:10	13	6	5	Proliferative
Male	58	01:50	14	10	4	Proliferative
Male	45	03:30	9	6	5	Exudative
Male	45	05:15	13	10	2	None
Female	50	02:15	3	2	2	Exudative

and hypertension were present in five (19.23%), hypertension and ischaemic heart disease in two (7.69%), and hypertension and chronic kidney disease in two patients (7.69%). One patient had diabetes mellitus, hypertension, and ischaemic heart disease, another had diabetes mellitus, hypertension and chronic kidney disease and yet another had suspected tertiary syphilis, hypertension, chronic kidney disease along with a past history of abdominal tuberculosis.

All 33 patients required oxygen administration at some point during hospitalization; of whom for 30 patients (90.91%), oxygen administration was inevitable at the time of admission. Among these 30

patients, oxygen was administered by nasal cannula or non-rebreather mask (NRBM) in 25 patients (83.33%), by high flow nasal cannula (HFNC) in one patient and by bilevel positive airway pressure (BiPAP) in four patients (13.33%). The other three patients were initially on room air. Ultimately, 28 of the 33 patients had to be shifted to invasive modes of ventilation, as their condition deteriorated gradually. The median duration for mechanical ventilation was three days (range 0-16 days).

In all 33 patients, antibiotics (azithromycin, levofloxacin, ceftriaxone, meropenem, piperacillin), anticoagulants (aspirin, enoxaparin, heparin) and steroids (methyl prednisolone, dexamethasone) were administered. Six patients (18.18%) received convalescent plasma. An antiviral medication (ramdesivir) was administered to 20 patients (60.61%), and an immunosuppressive medication (tocilizumab) was administered to 10 patients (30.3%).

To relate the laboratory investigations and autopsy findings, the last available laboratory report before death was taken into consideration. The laboratory investigations are summarized in Table II. Table III summarizes important macroscopic and microscopic findings of all organs.

Lungs: On macroscopic examination, the lungs appeared heavy, oedematous and congested. The mean weights of the right and left lungs of all 33 patients were 696.61 g (range 232-1220 g) and 641.30 g (range 167-1074 g), respectively. The outer surface of the lungs had a patchy appearance, alternating pinkish and bluish-purple patches or pinkish and dark red patches in some cases (Fig. 1A). On cut sections of lungs, thrombi protruding out from vessels were found in 14 (42.42%) cases (Fig. 2A). Lungs showed focal consolidations on cut sections in some cases, consistent with bronchopneumonia.

On microscopic examination, DAD in the exudative or proliferative phase was present in 29 (87.88%) cases (Fig. 1B and C). Hyaline membrane, microthrombi, vascular congestion, intra-alveolar oedema, type II pneumocytes hyperplasia and alveolar haemorrhage were major findings of DAD (Fig. 1B-E). The presence of inflammatory cells, primarily lymphocytes that infiltrated into the alveolar septa (interstitial pneumonia), was also noteworthy (Fig. 1B). Macro and/or microthrombi were present within pulmonary vessels in all cases (Figs 1F and 2B). Marked granulocytic infiltration of bronchiole and adjacent alveoli – bronchopneumonia was present in 15 (45.45%) of cases (Fig. 1G). Two cases had lung abscesses (Fig. 1H). There was a marked foreign body type giant cell reaction suggestive of aspiration pneumonia in one patient. The presence of pre-existent diseases such as tuberculous granulomas and emphysematous changes was recorded in a few patients.

Bacteria and fungi were isolated from lung tissue in 11 (33.33%) and pleural fluid in three (9.09%) cases. No organism was isolated from blood culture. Among the 11 cases where organisms were isolated from lung tissues, nine were found to have bronchopneumonia and two lung abscesses. In these nine cases of bronchopneumonia, *Acinetobacter* was isolated in three, *Klebsiella pneumoniae* in two, *Escherichia coli* in two, *Staphylococcus aureus* in one, and *Candida* in one. In addition, *K. pneumoniae*, *S. aureus*, and *E. coli* were also isolated from the pleural fluid of three of these nine cases. An antemortem diagnosis of bacterial infection was made only in one patient who had complained of purulent sputum; Gram-negative bacteria were found in his sputum microscopy. A lung abscess was discovered at autopsy in this case and microbial culture of lung tissue identified *Pseudomonas aeruginosa*. In another case of lung abscess, *Pseudomonas* and *K. pneumoniae* were isolated from the lung tissue.

Heart: On macroscopic examination, cardiomegaly was observed in 19 cases (57.58%). The mean weight (n=33) of the heart was 374.84 g (range 207-582 g). Massive cardiomegaly was found in one case with a weight of 582 g. The patient was suspected of having tertiary syphilis, according to his medical records. His two-dimensional echocardiographic report showed severe aortic regurgitation, aortic root dilatation, mild mitral regurgitation and moderate tricuspid regurgitation. The ventricular wall thickness measured one cm below the mitral/tricuspid valve ranged from 12 to 26 mm on the left and from 3 to 9 mm on the right. One case showed the presence of whitish hard calcified material over the tricuspid and mitral valve.

On microscopic examination, myocardial hypertrophy was the most common finding. Left ventricular hypertrophy was more common than right ventricular hypertrophy. Intramyocardial thrombus formation was observed in five (15.5%) cases (Fig. 2C).

Kidney: Macroscopically, kidneys were enlarged in 12 cases (36.36%). The mean weights (n=33) of the right and left kidneys were 135.76 g (range 80-189 g) and 133.48 g (range 78-209 g),

Table II. Summary of laboratory investigations in patients (n=33)

Investigation	Normal values	Number of cases for which reports were available	Number of cases where values were abnormal (%)	Average	Range	Interpretation
CRP	<6 mg/l	29	18 (62.07)	47.26	0.11-442.1	Increased
D-Dimer	<0.5 µg/ml	4	4 (100)	3.77	3.36->4	Increased
	<198 ng/ml	25	25 (100)	8669.04	204->32,000	Increased
IL-6	<7 pg/ml	17	7 (41.18)	431.83	5.8->4000	Increased
Ferritin	4.63-204 ng/ml	28	27 (96.43)	711.13	198.7->2000	Increased
LDH	230-460 IU/ml	8	6 (75)	865.12	299.93-1635	Increased
Procalcitonin	<0.05 ng/ml	6	4 (66.67)	0.43	0.05-2.12	Increased
Platelet	1.5-4.1 lac/µl	30	10 (33.33)	2.05	0.52-5.02	Decreased in 9 cases Increased in 1 case
WBC	4000-10,000 cells/µl	30	24 (80)	18,215	6480-45,300	Increased
Neutrophil	40-80	30	26 (86.67)	87.50	63-94	Increased
Lymphocyte	20-40	30	28 (93.33)	9.37	4-32	Decreased
NLR	1-3	31	29 (93.55)	12.42	1.97-23.50	Increased
Serum creatinine	0.57-1.11 mg/dl	29	12 (41.38)	2.13	0.5-14.3	Increased
Blood urea	10-45 mg/dl	27	19 (70.37)	84.26	17-265	Increased
Serum albumin	3.5-5.2 g/dl	23	18 (78.26)	3.17	2.6-3.7	Decreased
Total protein	6.4-8.3 g/dl	23	11 (47.83)	6.37	5.2-8.1	Decreased
Alkaline phosphatase	40-150 U/l	27	5 (18.52)	90.33	16-174	Decreased in 3, Increased in 2 cases
ALT	0-55 U/l	29	4 (14.29)	44.59	9-295	Increased
Direct bilirubin	0.0-0.5 mg/dl	29	3 (10.35)	0.40	0.2-2.1	Increased
Total bilirubin	0.2-1.2 mg/dl	29	1 (3.45)	0.74	0.3-3.2	Increased
Na+	136-145 mmol/l	27	17 (62.96)	135.55	121-150	Decreased in 14, Increased in 3 cases
K+	3.5-5.1 mmol/l	26	12 (46.15)	5.41	3.6-8.1	Increased
CK-MB	0-24 IU/l	5	5 (100)	74.5	36-131	Increased

NLR, neutrophil to lymphocyte ratio; CRP, C-reactive protein; IL-6, interleukin-6; LDH, lactate dehydrogenase; WBC, white blood cell count; ALT, alanine aminotransferase; CK-MB, creatine kinase-MB

respectively. Microscopically, the most prominent findings were acute tubular injuries, the main characteristics of which were dilation of the tubular lumen, flattening of tubular epithelium, focal tubular necrosis and hyaline granular cast (Fig. 3A). Seven (21.21%) cases showed fibrin thrombi in glomerular capillaries (Fig. 3B). Occasionally, thrombus within renal vessels was also seen (Fig. 2D). Pre-existent diseases such as benign cystic lesion, diabetic nephropathy, hypertensive nephropathy and chronic pyelonephritis were present in few patients (Fig. 3C-F).

Liver: The mean weight (n=33) of the liver was 1427.72 g (range 1256-1543 g). On microscopic examination, macrovesicular and microvesicular type of hepatic steatosis was found in almost all the patients located predominantly in the pericentral areas and to a lesser extent in periportal areas (Fig. 4A). A mild-to-moderate lymphocytic infiltrate was found in the portal area (Fig. 4B). A focal necrosis of hepatocytes was also observed without significant inflammation in a few cases (Fig. 4C). Steatohepatitis was present in few cases (Fig. 4D).

Brain: The mean weight (n=33) of the brain was 1127.58 g (range 937-1392 g). The brain did not exhibit any significant macroscopic or microscopic changes.

Table III. Major macroscopic and microscopic findings in different organs

Organ	Autopsy findings	Number (%) of cases
Lungs	Macroscopic findings	
	Pulmonary oedema	30 (90.91)
	Haemorrhagic surface	20 (60.61)
	Pleural adhesions	11 (33.33)
	Thrombi in pulmonary vessels	14 (42.42)
	Lung abscess	2 (6.06)
	Microscopic findings	
	Diffuse alveolar damage - Exudative phase	9 (27.27)
	Diffuse alveolar damage - Proliferative phase	20 (60.61)
	Hyaline membrane	29 (87.88)
	Hyperplasia of type II pneumocytes	20 (60.61)
	Microthrombi	33 (100)
	Macrothrombi	15 (45.45)
	Pulmonary capillary congestion	33 (100)
	Intra-alveolar and interstitial oedema	21 (63.64)
	Pigmented macrophages	13 (39.40)
	Haemorrhagic changes	33 (100)
	Multinucleated foreign body giant cells (aspiration pneumonia)	1 (3.03)
	Secondary bacterial infection	
	Bronchopneumonia	15 (45.45)
	Abscess formation	2 (6.06)
	Preexistent diseases	
	Emphysema	4 (12.12)
	Tuberculous granuloma	1 (3.03)
Heart	Macroscopic findings	
	Cardiomegaly	19 (57.58)
	Microscopic findings	
	Thrombus formation	5 (15.15)
	Focal myocardial necrosis	1 (3.03)
	Preexistent diseases	
	Left ventricular wall hypertrophy	23 (69.70)
	Right ventricular wall hypertrophy	14 (42.42)
	Calcification of mitral and tricuspid valves	1 (3.03)
	Fibrocollagenous band (a sign of old healed infarct)	1 (3.03)
	Atherosclerosis in aorta, left and right coronary artery	33 (100)
Kidney	Macroscopic findings	
	Granular surface	7 (21.21)
	Fluid filled cysts	6 (18.18)
	Renal stone	1 (3.03)
	Microscopic findings	
	Acute tubular injury	21 (63.64)

Contd...

Organ	Autopsy findings	Number (%) of cases
Kidney	Renal capillary congestion	33 (100)
	Focal haemorrhagic changes	33 (100)
	Small fibrin thrombi in glomerular capillaries	7 (21.21)
	Renal vascular thrombus	3 (9.09)
	Preexistent diseases	
	Tubular atrophy, chronic interstitial inflammation, interstitial fibrosis	12 (36.36)
	Nodular glomerulosclerosis (diabetic nephropathy)	4 (12.12)
	Hyaline arteriolosclerosis (hypertensive nephropathy)	8 (24.24)
	Thyroidization of tubules (chronic pyelonephritis)	14 (42.42)
Liver	Microscopic findings	
	Steatosis	29 (87.87)
	Periportal lymphocytic infiltrates	9 (27.27)
	Steatohepatitis	4 (12.12)
	Cholestasis	11 (33.33)
	Necrosis of hepatocytes	7 (21.21)
	Sinusoidal congestion	33 (100)
Brain	Macroscopic findings	
	Intracerebral haemorrhage	1 (3.03)
	Microscopic findings	
	Haemorrhagic changes without necrosis or inflammation in cerebrum	1 (3.03)
Spleen	Microscopic findings	
	Congestion and haemorrhage	33 (100)
	Lymphoid depletion in white pulp	4 (12.12)

Spleen: The spleen was enlarged in six cases (18.18%) and decreased in size in 15 (45.45%). The mean weight of the spleen (n=33) was 139.12 g (range 34-342 g). Upon microscopic examination, four cases showed lymphoid hypoplasia shown in Figure 5A, which contrasts with Figure 5B, which displayed normal white pulp.

Table IV shows the association between significant microscopic findings and duration of illness. The median duration of illness was six days (range 3-10 days) in cases of exudative DAD, 13 days (range 7-21 days) for proliferative DAD, 12 days (range 6-21 days) for bronchopneumonia and 13 days (range 3-19 days) for acute tubular necrosis.

Discussion

Our study revealed evidence of multi-organ dysfunction, thromboembolic events and hyperinflammatory state manifested by elevated inflammatory markers[20,21], such as white cell count, neutrophil to lymphocyte ratio, C-reactive protein, interleukin-6, lactate dehydrogenase, and ferritin. Studies have revealed that SARS-CoV-2 infects human cells by binding its spike protein to angiotensin-converting enzyme 2 (ACE2), which is widely expressed in several tissues like upper airways, lungs (type I and II pneumocytes), liver (cholangiocytes), intestines (enterocytes), heart (cardiomyocytes), kidney (proximal tubular epithelial cells), brain (neurons, astrocytes), blood vessels (endothelial cells, vascular smooth muscles), adipose tissue and reproductive organs (testis, vas deferens, ovaries). Along with SARS-CoV-2-induced cytotoxicity in these ACE2-expressing cells, several other mechanisms can cause multi-organ dysfunction in COVID-19[22].

The lungs bore most of the burden of COVID-19 in our study, similar to previous studies[5-15]. A prominent finding in our study was DAD, a histological feature of acute respiratory distress syndrome. It has three phases – an exudative phase that usually appears within 1-7 days, a proliferative phase, generally evident by 1 to 3 wk and fibrotic phase, typically seen after

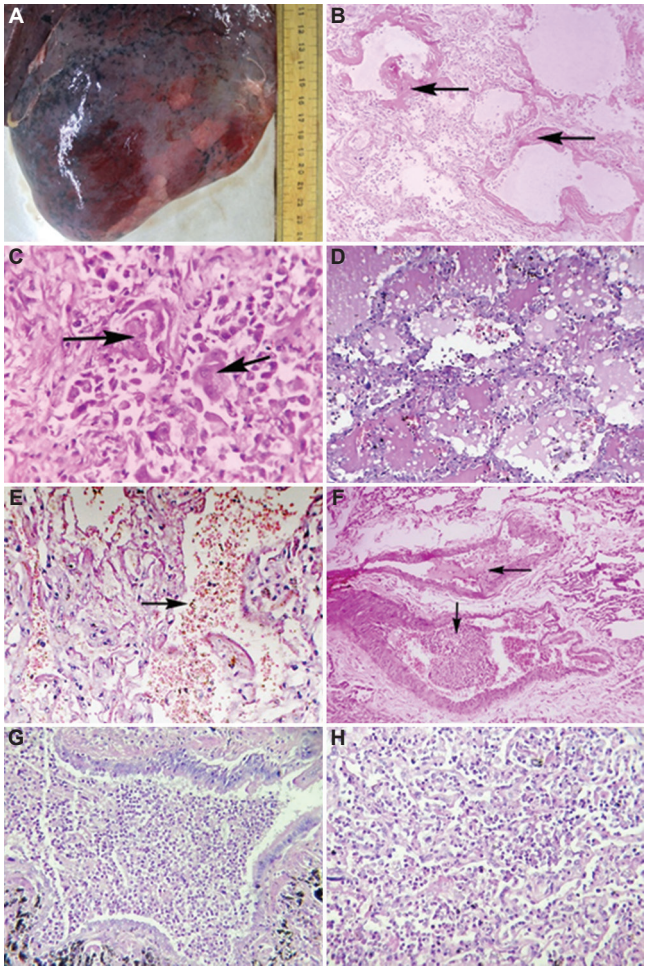

Fig. 1. Macroscopic and microscopic findings of the lungs. (**A**) An oedematous and haemorrhagic outer surface with patchy areas. (**B**) Exudative Diffuse Alveolar Damage – Hyaline membrane (black arrows) and mononuclear inflammatory cells in alveolar septa. (**C**) Proliferative Diffuse Alveolar Damage – Type 2 pneumocytes hyperplasia (black arrow). (**D**) Intraalveolar oedema. **(E)** Intraalveolar haemorrhage (black arrow).(**F**) Thrombi within segmental branches of the pulmonary artery (black arrows) (**G**) Bronchopneumonia showing abundant acute inflammatory cells. (**H**) Lung abscess showing acute inflammatory cells with necrotic debris. (B-H, H and E, ×40).

three weeks of illness[23]. The prevalence of proliferative DAD was higher than that of exudative DAD in our study. The fibrotic phase was not observed, which was consistent with illness duration being no longer than three weeks in each case.

Like other studies[5-10,12,15], we found microscopic and macroscopic evidence of secondary respiratory infections in the form of bronchopneumonia and lung abscesses, which were also supported by microbial cultures of pleural fluid and lung tissues as well as elevated procalcitonin levels. Such nosocomial infections among COVID-19 patients

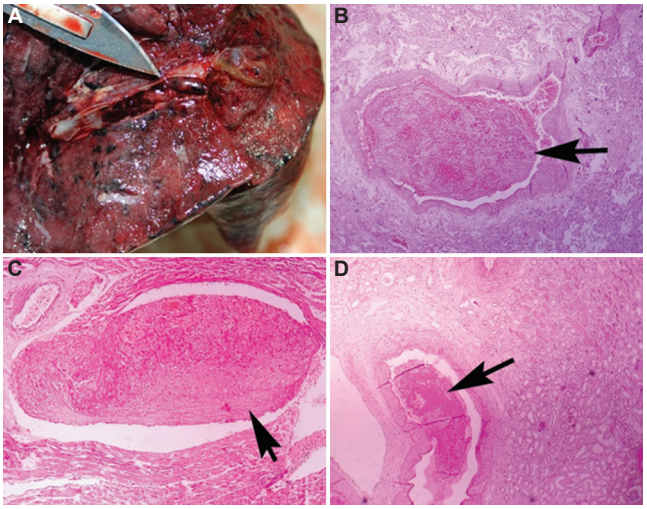

Fig. 2. Macroscopic and microscopic thrombi in various organs. (**A**) Thrombus adherent to vascular wall in a cut section of lung. (**B**) Pulmonary vascular thrombus (H and E, ×40). (**C**) Intramyocardial thrombus (H and E, ×40). (**D**) Renal vascular thrombus, (H and E, ×10).

could be caused by prolonged hospitalization, prolonged mechanical ventilation, central venous catheter usage, immunosuppressive medications like steroids and tocilizumab, as well as potential lapses in routine infection-prevention measures due to overburdened hospitals in this pandemic[24]. Accordingly, bronchopneumonia was found in seven of 10 patients treated with tocilizumab in our study. The mean duration of hospitalization as well as mechanical ventilation was higher among patients with nosocomial infections (7.76 and 5.06 days) than among the others (5.93 and 3.38 days). Five of seventeen patients with secondary infections had diabetes mellitus, which could have contributed to secondary infection.

We found evidence of thromboembolism in the form of thrombi in the lungs, heart and kidneys, along with the elevated d-dimer levels and thrombocytopenia. Several studies have reported the presence of thrombi in the lungs, heart, kidney, liver, spleen, brain and deep veins of the lower limbs[5,6,9,10,12-15].

The cardiovascular manifestations witnessed in COVID-19 patients include myocarditis, myocardial injury, arrhythmia, cardiac arrest, heart failure and coagulation abnormalities[6,11-13,15,25]. We observed myocardial thrombi and pathologies like ventricular hypertrophy and old infarct. Clinical records showed that creatine kinase-MB (CK-MB) levels were elevated in five patients who complained of chest pain; however, no recent myocardial infarction was found in these cases. Five patients suffered from heart failure

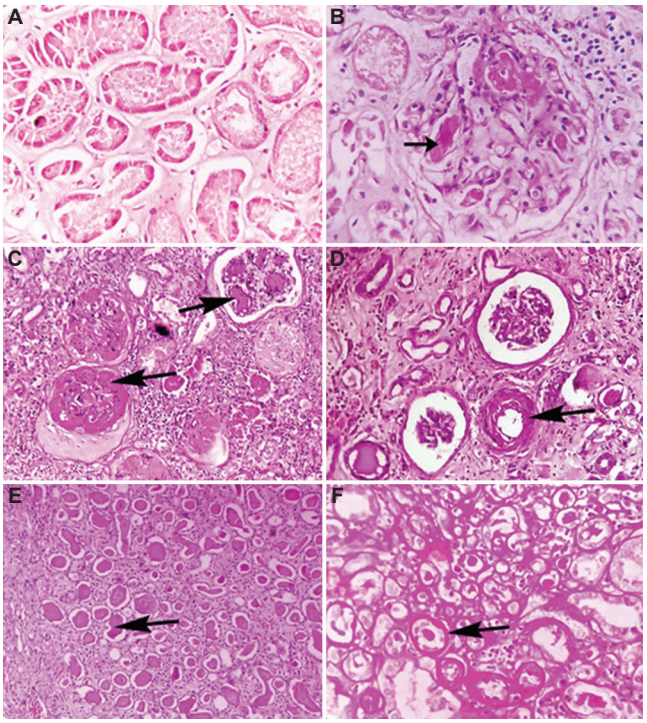

Fig. 3. Microscopic findings of the kidneys. (**A**) Acute tubular injury – Flattened and necrosed tubular epithelium with intratubular cast (H and E, ×40). (**B**) Fibrin thrombi within glomerular capillaries (black arrow) (H and E, ×40). (**C**) Nodular glomerulosclerosis (black arrows) (PAS, ×40). (**D**) Hyaline arteriolosclerosis (black arrow) (H and E, ×40). (**E**) Thyroidization of tubules (black arrow) (H and E, ×10). (**F**) Atrophic tubules with thickened basement membrane (black arrow), (PAS, ×10).

during hospitalization; each had co-morbid conditions of hypertension and ischaemic heart disease. This could be due to aggravation of pre-existing conditions by COVID-19.

In line with other studies[5,7,10,12,14,15], we found evidence of acute kidney injury in the form of acute tubular injury and altered renal functions, such as elevated serum creatinine, urea and potassium levels as well as decreased albumin, total protein and sodium levels. Besides viral pathogenesis, nephrotoxic drugs such as remdesivir and chloroquine may be involved in acute kidney injury[26].

The predominant hepatic findings in our study were sinusoidal congestion, steatosis, steatohepatitis and hepatocyte necrosis, as reported elsewhere[5,7,13,14]. Liver function tests were altered in five cases only. Steatosis may be caused by dysregulations in host lipid metabolism and mitochondrial activity resulting from virus-mediated cytotoxicity and cytokine storms, as well as side effects of drugs, including steroids and antivirals[27].

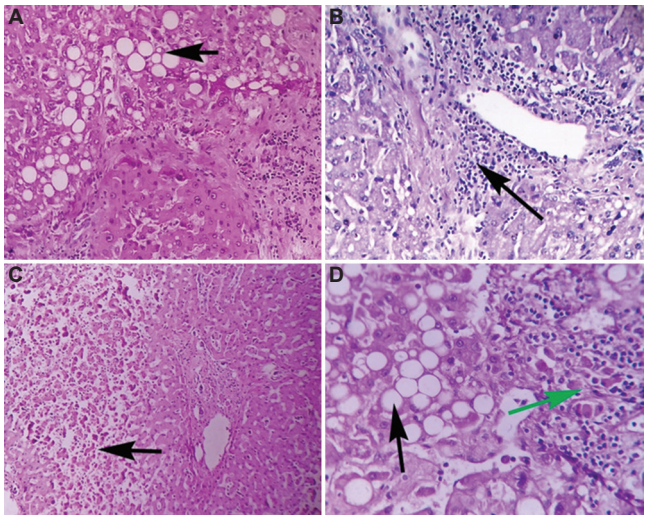

Fig. 4. Microscopic findings of the liver. (**A**) Microvesicular steatosis (black arrow) (H and E, ×10). (**B**) Periportal inflammatory infiltrates (black arrow) (H and E, ×40). (**C**) Focal necrosis of hepatocytes (black arrow) (H and E, ×10). (**D**) Steatohepatitis - Fatty vacuoles (black arrow) with inflammatory cells (green arrow), (H and E, ×40).

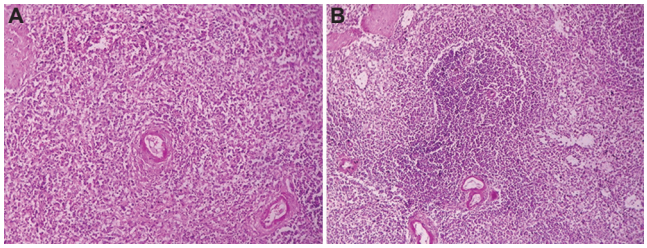

Fig. 5. Microscopic findings of the spleen. (**A**) Lymphoid hypoplasia in white pulp (H and E, ×10).(**B**) Normal white pulp (H and E, ×10).

Significant splenic findings in our study were decrease in size and lymphoid hypoplasia in the white pulp like in other studies[7,10,12]. Several mechanisms have been proposed to explain lymphopenia – viral and immune-mediated damage to lymphocytes, viral-mediated bone marrow impairment and thymus suppression, redistribution of lymphocyte to lungs and gastrointestinal tract and biochemical changes (elevated bilirubin, creatinine and lactic acid) mediated decreased production and survival of lymphocytes[28].

No significant COVID-19-related histological findings were observed in the brain. Some studies have reported severe inflammatory response in the CNS, as evidenced by microglial activation, astrogliosis and perivascular cuffing of T-cells[12,15]. As reported in other studies[5-15], pulmonary pathology – DAD complicated by bronchopneumonia/lung abscess and pulmonary thromboembolism was the most common cause of death among our study participants.

Table IV. Association between significant microscopic findings and the duration of illness

Microscopic finding	Number (%) of cases in duration of illness			Total number of cases
	1-7 days	8-14 days	>14 days	
Significant pulmonary microscopic findings				
Diffuse alveolar damage - Exudative phase	5 (55.56)	4 (44.44)	0	9
Diffuse alveolar damage - Proliferative phase	1 (5)	14 (70)	5 (25)	20
Bronchopneumonia	2 (13.33)	11 (78.33)	2 (13.33)	15
Lung abscess	0	2 (100)	0	2
Significant renal microscopic findings				
Acute tubular necrosis	4 (19.05)	13 (61.90)	4 (19.05)	21
Significant splenic microscopic findings				
Lymphoid depletion in white pulp	1 (25)	2 (50)	1 (25)	4
Evidence of thromboembolism				
Pulmonary microthrombi	8 (24.24)	19 (57.58)	6 (18.18)	33
Pulmonary macrothrombi	2 (13.33)	10 (66.67)	3 (20)	15
Intramyocardial thrombi	4 (80)	1 (20)	0	5
Thrombi in glomerular capillaries	2 (28.57)	4 (57.14)	1 (14.29)	7
Renal vascular thrombi	0	2 (66.67)	1 (33.33)	3

The exudative phase of DAD was frequently found with shorter durations of illness (less than a week), whereas the proliferative phase was observed with longer durations (more than a week). Acute kidney injury, secondary respiratory infections and pulmonary macrothrombi were common with more than one week of illness. The number of cases was not sufficient to correlate other autopsy findings with length of illness.

There were certain limitations in our study. We approached relatives of several deceased, but only a few of them consented. That led to a relatively small sample size. The deep veins of the lower limb and the gut were not examined. The presence of the virus was not examined in various organs as immunohistochemistry was not available.

In conclusion, the predominant findings of COVID-19 in our study were DAD (features of acute respiratory distress syndrome), acute tubular injury (features of acute kidney injury), and hypercoagulability, characterized by the presence of thrombi in multiple organs. These findings along with altered laboratory investigations correspond with immune-mediated cellular injury along with direct virus-mediated cellular damage.

***Financial support & sponsorship*:** None.

***Conflicts of Interest*:** None.

References

1. Jin Y, Yang H, Ji W, Wu W, Chen S, Zhang W, *et al*. Virology, epidemiology, pathogenesis, and control of COVID-19. *Viruses* 2020; *12* : 372.
2. Amawi H, Abu Deiab GI, A Aljabali AA, Dua K, Tambuwala MM. COVID-19 pandemic: An overview of epidemiology, pathogenesis, diagnostics and potential vaccines and therapeutics. *Ther Deliv* 2020; *11* : 245-68.
3. Barth RF, Xu X, Buja LM. A call to action: The need for autopsies to determine the full extent of organ involvement associated with COVID-19. *Chest* 2020; *158* : 43-4.
4. Pomara C, Li Volti G, Cappello F. COVID-19 deaths: Are we sure it is pneumonia? Please, autopsy, autopsy, autopsy! *J Clin Med* 2020; *9* : 1259.
5. Menter T, Haslbauer JD, Nienhold R, Savic S, Hopfer H, Deigendesch N, *et al*. Postmortem examination of COVID-19 patients reveals diffuse alveolar damage with severe capillary congestion and variegated findings in lungs and other organs suggesting vascular dysfunction. *Histopathology* 2020; *77* : 198-209.
6. Wichmann D, Sperhake JP, Lütgehetmann M, Steurer S, Edler C, Heinemann A, *et al*. Autopsy findings and venous thromboembolism in patients with COVID-19: A prospective cohort study. *Ann Intern Med* 2020; *173* : 268-77.
7. Lax SF, Skok K, Zechner P, Kessler HH, Kaufmann N, Koelblinger C, *et al*. Pulmonary arterial thrombosis in COVID-19 with fatal outcome: Results from a prospective, single-center, clinicopathologic case series. *Ann Intern Med* 2020; *173* : 350-61.

8. Youd E, Moore L. COVID-19 autopsy in people who died in community settings: The first series. *J Clin Pathol* 2020; *73* : 840-4.

9. Carsana L, Sonzogni A, Nasr A, Rossi RS, Pellegrinelli A, Zerbi P, *et al*. Pulmonary post-mortem findings in a series of COVID-19 cases from northern Italy: A two-centre descriptive study. *Lancet Infect Dis* 2020; *20* : 1135-40.

10. Rapkiewicz AV, Mai X, Carsons SE, Pittaluga S, Kleiner DE, Berger JS, *et al*. Megakaryocytes and platelet-fibrin thrombi characterize multi-organ thrombosis at autopsy in COVID-19: A case series. *EClinicalMedicine* 2020; *24* : 100434.

11. Schaller T, Hirschbühl K, Burkhardt K, Braun G, Trepel M, Märkl B, *et al*. Postmortem examination of patients with COVID-19. *JAMA* 2020; *323* : 2518-20.

12. Hanley B, Naresh KN, Roufosse C, Nicholson AG, Weir J, Cooke GS, *et al*. Histopathological findings and viral tropism in UK patients with severe fatal COVID-19: A post-mortem study. *Lancet Microbe* 2020; *1* : e245-53.

13. Falasca L, Nardacci R, Colombo D, Lalle E, Di Caro A, Nicastri E, *et al*. Postmortem findings in Italian patients with COVID-19: A descriptive full autopsy study of cases with and without comorbidities. *J Infect Dis* 2020; *222* : 1807-15.

14. Elsoukkary SS, Mostyka M, Dillard A, Berman DR, Ma LX, Chadburn A, *et al*. Autopsy findings in 32 patients with COVID-19: A single-institution experience. *Pathobiology* 2021; *88* : 56-68.

15. Schurink B, Roos E, Radonic T, Barbe E, Bouman CS, de Boer HH, *et al*. Viral presence and immunopathology in patients with lethal COVID-19: A prospective autopsy cohort study. *Lancet Microbe* 2020; *1* : e290-9.

16. Newer Additional Strategies for COVID-19 Testing. Indian Council of Medical Research. New Delhi, India. Available from: *https://www.icmr.gov.in/pdf/covid/strategy/New_additional_Advisory_23062020_3.pdf,* accessed on May 30, 2021.

17. COVID-19: Guidelines on Dead Body Management. Directorate General of Health Services, Ministry of Health & Family Welfare, Government of India. Available from: *https://www.mohfw.gov.in/pdf/1584423700568_COVID19GuidelinesonDeadbodymanagement.pdf,* accessed on February 18, 2021.

18. Indian Council of Medical Research. *Standard guidelines for medico-legal autopsy in covid-19 deaths in India*. Available from: *https://stopcorona.tn.gov.in/wp-content/uploads/2020/03/Standard-guidelines-for-Medico-legal-autopsy-in-COVID-19-deaths-in-India-10.05.2020-32-Pages-English-1.07-MB.pdf*, accessed on January 1, 2022.

19. Centers for Disease Control and Prevention. *Collection and submission of postmortem specimens from deceased persons with known or suspected COVID-19*. Available from: *https://www.cdc.gov/coronavirus/2019-ncov/hcp/guidance-postmortem-specimens.html,* accessed on February 18, 2021.

20. Hariyanto TI, Japar KV, Kwenandar F, Damay V, Siregar JI, Lugito NP, *et al*. Inflammatory and hematologic markers as predictors of severe outcomes in COVID-19 infection: A systematic review and meta-analysis. *Am J Emerg Med* 2021; *41* : 110-9.

21. Deng F, Zhang L, Lyu L, Lu Z, Gao D, Ma X, *et al*. Increased levels of ferritin on admission predicts intensive care unit mortality in patients with COVID-19. *Med Clin (Barc)* 2021; *156* : 324-31.

22. Lopes-Pacheco M, Silva PL, Cruz FF, Battaglini D, Robba C, Pelosi P, *et al.* Pathogenesis of multiple organ injury in COVID-19 and potential therapeutic strategies. *Front Physiol* 2021; *12* : 593223.

23. Yoshikawa A, Fukuoka J. ARDS/DAD. PathologyOutlines.com website. Available from: *https://www.pathologyoutlines.com/topic/lungnontumordiffusealveolardamage.html,* accessed on February 18, 2021.

24. Rawson TM, Wilson RC, Holmes A. Understanding the role of bacterial and fungal infection in COVID-19. *Clin Microbiol Infect* 2021; *27* : 9-11.

25. Kwenandar F, Japar KV, Damay V, Hariyanto TI, Tanaka M, Lugito NP, *et al*. Coronavirus disease 2019 and cardiovascular system: A narrative review. *Int J Cardiol Heart Vasc* 2020; *29* : 100557.

26. Izzedine H, Jhaveri KD. Acute kidney injury in patients with COVID-19: An update on the pathophysiology. *Nephrol Dial Transplant* 2021; *36* : 224-6.

27. Nardo AD, Schneeweiss-Gleixner M, Bakail M, Dixon ED, Lax SF, Trauner M. Pathophysiological mechanisms of liver injury in COVID-19. *Liver Int* 2021; *41* : 20-32.

28. Jafarzadeh A, Jafarzadeh S, Nozari P, Mokhtari P, Nemati M. Lymphopenia an important immunological abnormality in patients with COVID-19: Possible mechanisms. *Scand J Immunol* 2021; *93* : e12967.

For correspondence: Dr Pratik R. Varu, Department of Forensic Medicine, Pandit Deendayal Upadhyay Government Medical College, Civil Hospital Campus, Jamnagar Road, Rajkot 360 001, Gujarat, India
e-mail: drpratik5388@gmail.com